A GREY-BOX MODELLING APPROACH FOR THE NONLINEAR PARAMETRIC CHANNEL

Karsten Wiedmann and Tobias Weber

Institute of Communications Engineering, University of Rostock
Richard-Wagner-Str. 31, 18119 Rostock, Germany
Email: {karsten.wiedmann}{tobias.weber}@uni-rostock.de

ABSTRACT

Parametric transduction systems employ the nonlinear propagation of acoustic waves in fluid media. The nonlinear effects are beneficially used, which is in contrast to classic communication approaches. In this paper, a point-to-point model for the underlying parametric channel is investigated using a grey-box modelling approach. Prior knowledge is derived from a physical modelling.

As a result, a block-oriented model is derived that consists of the concatenation of a static nonlinearity and a dynamic linearity. The structure belongs to the class of Hammerstein-Models, which are commonly used in nonlinear system modelling. In contrast to a black-box approach, the derived model simplifies parameter identification significantly and supports the design of high performance parametric communication systems.

Finally, measurement results which are in good agreement with the derived model are reported.

Index Terms— nonlinear channel modelling , Parametric Communication System, parametric transduction

1. INTRODUCTION

The propagation of acoustic waves in fluid media is a nonlinear process. Especially in high power scenarios, nonlinear effects cannot be neglected.

Communication systems usually suffer from nonlinearity and performance degrades with rising nonlinear effects such as the Kerr effect in optical communications [1] or power amplifier distortions in satellite communications [2]. Since these systems focus on pure linear wave propagation, a variety of techniques to overcome or at least minimise nonlinear distortions have been developed in the certain fields.

Contrarily, particular communication systems employ nonlinear wave propagation and use nonlinear effects beneficially, for instance sub button profiling [3, 4], parametric underwater communications [5, 6, 7, 8], virtual microphones [9] or the audio spotlight [10]. These systems are based on the parametric array [11]. For this, an appropriately modulated high frequency acoustic wave, called primary wave, is transmitted. Because of its high centre frequency, the primary wave features a high directivity and a high absolute bandwidth enabling ultra-wideband modulation. During nonlinear wave propagation, intermodulation within the transmitted primary wave takes place. As a result, a secondary wave of new frequencies is generated, which possess low frequency components. These low frequency components feature nearly the same high directivity and the same absolute bandwidth as the transmitted primary wave. In this way, a modulated wave with favourable properties can be generated.

A variety of applications are discussed in literature, but only little investigations concerning the underlying nonlinear channel from the theoretical point of view can be found. Since a proper channel model is inevitable for the design of high performance parametric systems, a point-to-point model for the nonlinear parametric channel is established in this paper.

The investigation of nonlinear models is basically challenging and solutions have to be found for the particular scenarios. A black-box approach, as it was reported for the parametric channel in [12], does not consider any knowledge about the physical process. Consequently, corresponding models feature a high complexity, give only little understanding about the internal behaviour, usually need a severe identification effort and their accuracy depends strongly on the acquired measurements. A complete white-box approach on the other hand is highly complex and corresponding approaches suffer from assumptions.

For these reasons, a grey-box modelling approach is discussed in this paper. The obtained model is physically motivated and hence gives qualitative knowledge about the internal behaviour of the nonlinear propagation process. This supports the system design, e.g. the finding of appropriate modulation schemes or the investigation of appropriate identification methods.

The prior knowledge is obtained from a physical modelling discussed in Sec. 2. As a result, a block-oriented model that consists of the concatenation of a static nonlinearity and a dynamic linearity is established in Sec. 3. Finally, a parametric transmission system is applied to validate the derived model. The results are discussed in Sec. 4. The paper concludes in Sec. 5.

978-1-4799-2893-4/14/$31.00 ©2014 IEEE

2. PHYSICAL MODELLING

2.1. Basic equation set

A physical modelling of the wave propagation in fluid media is briefly summarized to generate prior knowledge. For this purpose, the fluid will be described by its intrinsic state variables, which are the local pressure $p = p_0 + \tilde{p}$, local density $\rho = \rho_0 + \tilde{\rho}$ and velocity $\mathbf{v}$. Here, p_0 and ρ_0 are equilibrium state variables in the quiescent fluid and $\tilde{p}$, $\tilde{\rho}$ and $\mathbf{v}$ are disturbances induced by a propagating wave.

Dependencies of these state variables are formulated in a basic equation set [13], which consists of the Euler equations

$$\frac{\partial \rho}{\partial t} = -\mathrm{div}\{\rho\,\mathbf{v}\} \tag{1}$$

$$\frac{\partial}{\partial t}\{\rho\,\mathbf{v}\} = -\left(\mathrm{div}\{\rho\mathbf{v}\cdot\mathbf{v}^{\mathrm{T}}\}\right)^{\mathrm{T}} - \mathrm{grad}\{p\}\ , \tag{2}$$

namely the equation of continuity and the equation of motion, as well as the equation of state for isentropic processes

$$\rho = \mathrm{f}(p)\ . \tag{3}$$

The equation set of (1)-(3) is commonly used in fluid dynamics and is accurate for ideal fluids, i.e. fluids with zero viscosity. Real fluids like water or air feature a low viscosity and are appropriately modelled using this equation set.

The equation of continuity (1) describes the conservation of mass in a compressible fluid flow. No further simplification is needed for the further modelling. The equation of motion (2) describes the conservation of momentum and features a second-order and a third-order nonlinear term. A second-order approximation to reduce complexity gives the approximation $\rho\mathbf{v}\cdot\mathbf{v}^{\mathrm{T}} \approx \rho_0\mathbf{v}\cdot\mathbf{v}^{\mathrm{T}}$. As a result, the vector identity

$$\left(\mathrm{div}\{\mathbf{v}\cdot\mathbf{v}^{\mathrm{T}}\}\right)^{\mathrm{T}} = \mathbf{v}\,\mathrm{div}\{\mathbf{v}\} + \frac{\mathrm{grad}\{v^2\}}{2} - \mathbf{v}\times\mathrm{rot}\{\mathbf{v}\} \tag{4}$$

can be substituted into (2). For ideal fluids that are initially at rest, the constraint $\mathrm{rot}\{\mathbf{v}\} = 0$ holds for every time instance. The discussed manipulations give the equation of motion

$$\frac{\partial}{\partial t}\{\mathbf{v}\,\rho\} \approx -\rho_0\,\mathbf{v}\,\mathrm{div}\{\mathbf{v}\} - \frac{\rho_0}{2}\mathrm{grad}\{v^2\} - \mathrm{grad}\{p\}\,. \tag{5}$$

To apply the second-order approximation on the equation of state, the nonlinear function in (3) is developed in a Taylor series and higher order nonlinear terms are neglected, giving

$$\rho(p) \approx \rho_0 + \sum_{n=1}^{2} \frac{1}{n!}\left.\frac{\partial^n \rho}{\partial p^n}\right|_{p=p} (p - p_0)^n\ . \tag{6}$$

2.2. Second-order wave equation

The second-order approximations of the basic equations can be substituted into one differential equation, reading after some manipulations

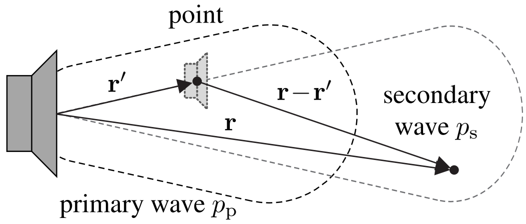

Fig. 1. Considered geometry.

$$\frac{1}{c_0^2}\frac{\partial^2\tilde{p}}{\partial t^2} - \Delta\tilde{p} = \rho_0\,\mathrm{div}\{\mathbf{v}\,\mathrm{div}\{\mathbf{v}\}\} + \rho_0\frac{1}{2}\Delta\,v^2 - \frac{\partial^2}{\partial t^2}\left\{\frac{1}{2}\frac{\partial^2\rho}{\partial p^2}\tilde{p}^2\right\}\ . \tag{7}$$

To simplify equation (7), the quasi-linear approach [14, 15] is applied. Here, the initially transduced wave is denoted as primary wave p_{p}. This primary wave is assumed to propagate mainly in a linear fashion for what reason its propagation is described by the linear approximation of the basic equation set (1)-(3) [15]. Due to the propagation in the nonlinear fluid, the primary wave is supposed to create virtual sources, see Fig. 1. These virtual sources are spatially distributed and radiate elementary waves of a so-called secondary wave p_{s}, which has new frequency components. Since it has a low power, the secondary wave is also assumed to propagate in a linear fashion but not to create any further nonlinear sources. As a result, the nonlinear terms on the right of (7) are only created by the primary wave p_{p} and the linear terms on the left describe the linear propagation of the nonlinearly generated secondary wave p_{s}.

Applying this and neglecting near field effects of the transducer, a manipulation by substituting the linear basic equations into the right side of (7) results in

$$\frac{1}{c_0^2}\frac{\partial^2 p_{\mathrm{s}}}{\partial t^2} - \Delta p_{\mathrm{s}} = \beta\frac{\partial^2 p_{\mathrm{p}}^2}{\partial t^2}\ , \tag{8}$$

with $\beta = \frac{1}{c_0^4\rho_0}\left(1 - \frac{c_0^4\rho_0}{2}\frac{\partial^2\rho}{\partial p^2}\right)$. The right side of (8) is the source strength density of the virtual sources. Equation (8) was first derived by Westervelt [11, 16] and will be used for the following channel modelling. For this, the wave equation (8) is transformed into the frequency domain, reading

$$\frac{(2\pi f)^2}{c_0^2}\,\underline{P}_{\mathrm{s}} + \Delta\underline{P}_{\mathrm{s}} = \beta(2\pi f)^2\left(\underline{P}_{\mathrm{p}} * \underline{P}_{\mathrm{p}}\right)\ . \tag{9}$$

3. CHANNEL MODELLING

3.1. Solution of the Wave Equation

In the following, the solution of the Westervelt equation is discussed to obtain prior knowledge for the channel modelling.

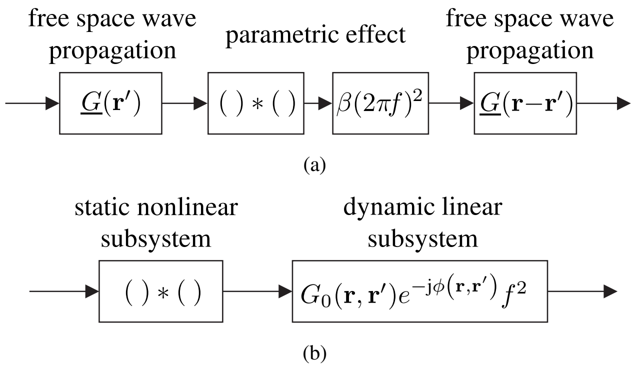

Fig. 2. Point-to-point model (a) and simplified model (b) for a single virtual source point.

The considered geometry is shown in Fig. 1. For simplification, the source that radiates the primary wave is considered as a point source at the origin having the source strength $\underline{Q}_{\mathrm{p}}(f)$. According to the quasi-linear approach, the primary wave mainly propagates in a linear fashion, giving at a certain point $\mathbf{r}'$ the primary wave

$$\underline{P}_{\mathrm{p}}(f,\mathbf{r}') = \underline{G}(\mathbf{r}')\,\underline{Q}_{\mathrm{p}}(f)\,, \tag{10}$$

where

$$\underline{G}(\mathbf{r}') = \frac{e^{-\mathrm{j}2\pi f r'/c}}{4\pi r'} \tag{11}$$

is Green's function according to the phase shift and the spherical spreading during the free space wave propagation [15]. The primary wave creates at the point $\mathbf{r}'$ a virtual source with the source strength density

$$\underline{q}(f,\mathbf{r}') = \beta(2\pi f)^2\left(\underline{P}_{\mathrm{p}} * \underline{P}_{\mathrm{p}}\right)(f,\mathbf{r}')\,. \tag{12}$$

The complete virtual source distribution radiates with the source strength density in (12), giving at a certain point $\mathbf{r}$ the secondary wave

$$\underline{P}_{\mathrm{s}}(f,\mathbf{r}) = \iiint_{V'} \underline{G}(\mathbf{r}-\mathbf{r}')\,\underline{q}(f,\mathbf{r}')\,\mathrm{d}\mathbf{r}'\,. \tag{13}$$

Substituting the equations (10)-(12) into (13) gives a relation between the transduced and the nonlinearly generated wave.

3.2. Channel Model for a Single Virtual Source Point

Based on the discussed solution in equation (13), a block-oriented channel model is derived in the following.

At start, only the presence of one virtual point source is considered, compare Fig. 1. For this, the point-to-point model shown in Fig. 2(a) can be motivated. The first block describes the linear propagation of the primary wave to the point $\mathbf{r}'$ according to equation (10). Then, a virtual source that radiates a wave proportional to the auto-convoluted primary wave is created by the primary wave at the point $\mathbf{r}'$, compare equation (12). This is modelled by the second and third block in Fig. 2(a). The fourth block finally describes the linear propagation of the secondary wave field to point $\mathbf{r}$.

The structure in Fig. 2(a) can be simplified. Considering a non-dispersive propagation velocity c, the order of the first and second block can be changed. For this, the linear block has to be multiplied by the factor $1/(4\pi r')$. The concatenated linear subsystems are then combined to one linear system, reading

$$\begin{aligned}\underline{G}_{\mathrm{g}}(f,\mathbf{r},\mathbf{r}') &= \frac{1}{4\pi r'}\underline{G}(\mathbf{r}')\beta(2\pi f)^2\underline{G}(\mathbf{r}-\mathbf{r}') \\ &= G_0(\mathbf{r},\mathbf{r}')e^{-\mathrm{j}\phi(\mathbf{r},\mathbf{r}')}f^2\end{aligned} \tag{14}$$

with the substitutions $G_0(\mathbf{r},\mathbf{r}') = \beta/(16\pi r'^2\,||\mathbf{r}-\mathbf{r}'||)$ and $\phi(\mathbf{r},\mathbf{r}') = 2\pi f\,(r' + ||\mathbf{r}-\mathbf{r}'||)\,/c$. The model parameters G_0 and ϕ can be fully determined as a function of the vectors $\mathbf{r}'$ and $\mathbf{r}$. Thus, the resulting model shown in Fig. 2(b) is a white-box model representing the exact solution in (13) of the wave equation (9) for one single source point.

3.3. Channel Model for the Complete Source Distribution

Considering the complete source distribution, the contributions of all virtual source points in the source volume have to be summed up, see equation (13). This means that an infinite number of single source point models shown in Fig. 2(b) have to be connected in parallel. The nonlinear blocks can simply be extracted to one block in front of the parallel branches. Nevertheless, this results in an undetermined model structure, because the linear subsystems induce different distortions in dependence on their particular virtual point source. Hence, a white-box approach is not straightforward any more.

For this reason, a grey-box modelling approach will be discussed in the following. The linear subsystems can be gathered and one system representing the overall linear distortion can be used instead. This leads to a model structure similar to the model shown in Fig. 2(b) but now with unknown parameters G_0 and ϕ. Nevertheless, the model gives qualitative knowledge about the parametric wave propagation process, i.e. the linear and nonlinear signal distortions. This enables the investigation of appropriate signal processing strategies in the particular fields of application without the determination of the exact solution in (13).

It can be seen, that the model consists of a concatenation of a static nonlinear and a dynamic linear subsystem. This is a major outcome of this modelling approach. In comparison to a dynamic nonlinear system, the presence of the static nonlinearity simplifies the signal processing effort significantly, e.g. for parameter identification. Moreover, the derived model structure is a special kind of the well investigated Hammerstein-Models [17] for what reason corresponding signal processing methods may be applicable for the case of parametric transduction.

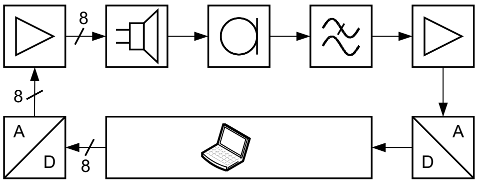

Fig. 3. Measurement setup.

4. VALIDATION

The results reported below support the derived model structure, especially the presence of a static nonlinearity.

The parametric transduction system depicted in Fig. 3 was used for the measurements. The primary signal is transduced by an acoustic transducer array consisting of 8x16 PROWAVE 400ST100 array elements. Each row, i.e. 16 array elements, can transmit a separate signal, which is generated by a desktop PC, subsequently D/A-converted and amplified. For the measurements, a sinusoid at $f_1 = 39.6\,\mathrm{kHz}$ was transmitted by four output channels and another sinusoid at $f_2 = 40.4\,\mathrm{kHz}$ was transmitted with the others. In this way, secondary components at $f_{\mathrm{diff}} = f_2 - f_1 = 0.8\,\mathrm{kHz}$ as well as at $f_{\mathrm{sum}} = f_1 + f_2 = 80\,\mathrm{kHz}$ are nonlinearly created during wave propagation, where possible contributions at these frequencies originating from amplifier nonlinearity are prevented. The resulting wave is received by a condenser microphone of the type Microtech Gefell MK301, low-pass filtered and amplified. Both the D/A-and the A/D-converter work at $250\,\mathrm{kHz}$ sampling frequency and are synchronised, so that the sound pressure level (SPL) for each frequency could be estimated using the least-squares algorithm.

Fig. 4(a) shows denoted by M_1 the estimated SPL vs. the distance r between the transducer array and the microphone. The waves are supposed to suffer a propagation loss due to spherical spreading and attenuation. Thus, extrapolation curves of the form $\mathrm{E}(f) = P_0(f) - 20\log_{10}(r) - r\,\alpha_{\mathrm{dB}}(f)$ with $P_0(f)$ and $\alpha_{\mathrm{dB}}(f)$ denoting the initial SPL and the attenuation coefficient at a certain frequency, respectively, are plotted to evaluate the measurement results. For the primary wave, the measurement results and the extrapolation curve are in a good agreement. Since the secondary wave is proportional to the squared primary wave, see equation (12) in the time domain, the secondary wave suffers twice the transmission loss of the primary wave within the active region of the parametric array. This is illustrated by the extrapolation curve $2\mathrm{E}(f_{1,2})$, where twice the transmission loss of the primary wave is considered at the initial SPL of the secondary component. In this scenario, the active region is about $4\,\mathrm{m}$, see Fig. 4(a). Beyond this region, no further significant primary sources exist and the secondary wave propagates in good agreement to $\mathrm{E}(f_{\mathrm{diff}})$. This shows that the observed parametric wave propagation can be properly explained by the physical modelling discussed in Sec. 2.

Furthermore, the SPL of the primary wave was varied and the SPLs of both the difference and sum frequency component were measured at a distance of $5\,\mathrm{m}$. Fig. 4(b) shows the results denoted by M_2. It can be seen that the SPLs of the secondary components increase linearly with an increase in the SPLs of the primary field. For reason of comparison, linear extrapolation curves denoted by L are plotted in Fig. 4(b) for both of the secondary components. The curves feature a slope equal to two, since the secondary wave is proportional to the squared primary wave. In a further measurement, a third sinusoid at $f_3 = 40.8\,\mathrm{kHz}$ was additionally transmitted by two of the output channels. The SPLs are again estimated and shown in Fig. 4(b) denoted by M_3. It can be seen that the obtained results are identical to the results of M_2. This shows that a change in the primary wave form does not influence the secondary wave generation at the measured frequencies. This behaviour is not expected when a significant dynamic nonlinear element is presence, which is sensitive to variations in the wave form. Consequently, the measurements indicate the presence of a static nonlinearity and a dynamic linearity in the parametric channel.

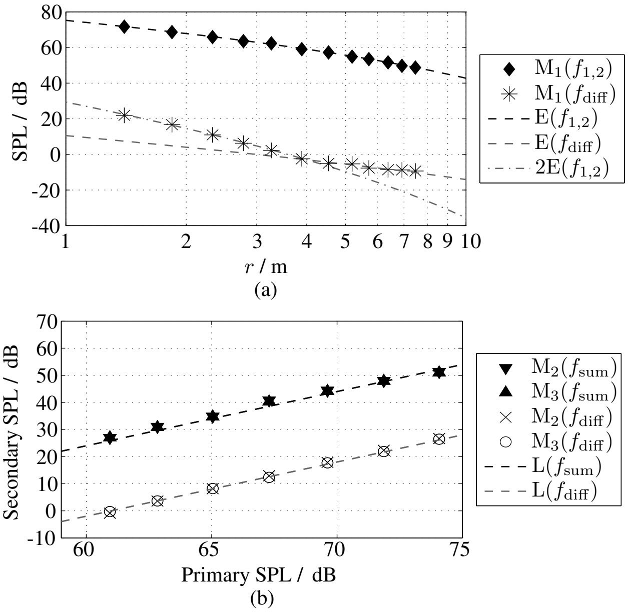

Fig. 4. Measurement results.

Further measurements with varying distances and frequencies confirmed this observation.

5. CONCLUSION

In this paper, a grey-box modelling approach for the nonlinear parametric channel was discussed. Starting from the physical modelling, a model that consists of a concatenation of a static nonlinear and a dynamic linear subsystem was established. Most notably is the presence of a static nonlinear system that simplifies the signal processing effort significantly.

First measurement results were reported which support the assumption of a static nonlinear element in the channel model. In future work, more extensive measurement campaigns have to be carried out to validate the derived model.

6. REFERENCES

[1] P. P. Mitra and J. B. Stark, "Nonlinear limits to the information capacity of optical fibre communications," *Nature*, vol. 411, pp. 1027–1030, 2001.

[2] P. Zillmann and G. P. Fettweis, "On the capacity of multicarrier transmission over nonlinear channels," *Proc. IEEE Vehicular Technology Conference*, vol. 2, pp. 1148 – 1152, 2005.

[3] Innomar Technologie GmbH, "Parametric technology for high resolution sub-buttom profiling," *Offshore Technology International*, vol. 01/09, pp. 83–84, 2009.

[4] O. Bergem and N.G. Pace, "Installation and calibration of a parametric array for shallow water backscatter measurement," *Proc. MTS/IEEE OCEANS '96*, vol. 2, pp. 773–777, 1996.

[5] R.F.W. Coates, M. Zheng, and L. Wang, "Bass 300 paracom: A model underwater parametric communication system," *IEEE Journal of Oceanic Engineering*, vol. 21, no. 2, pp. 225–232, 1996.

[6] G. Loubet and L. Kopp, "Parametric transmission of wide-band signals," *Proc. MTS/IEEE OCEANS '96*, vol. 2, pp. 839–844, 1996.

[7] A. Quazi and W. Konrad, "Underwater acoustic communications," *IEEE Communications Magazine*, vol. 20, no. 2, pp. 24–30, 1982.

[8] K. Wiedmann and T. Weber, "Constellation-constrained capacities for parametric underwater communication," *Proc. OCEANS'13 MTS/IEEE Bergen*, 2013.

[9] T. Merkel, H.-G. Lühmann, and T. Ritter, "Using ultrasonic sound to collect audio waves in air," *Journal of the Audio Engineering Society*, vol. 61, no. 9, pp. 656–666, 2013.

[10] M. Yoneyama, J. Fujimoto, Y. Kawamo, and S. Sasabe, "The audio spotlight: An application of nonlinear interaction of sound waves to a new type of loudspeaker design," *Journal of the Acoustical Society of America*, vol. 73, no. 5, pp. 1532–1536, 1983.

[11] P. J. Westervelt, "Parametric acoustic array," *Journal of the Acoustical Society of America*, vol. 35, no. 4, pp. 535–537, 1963.

[12] T. Buch and G. Wendt, "Modellierung des nichtlinearen Unterwasserkanals," *Tagungsband des 11. Symposium Maritime Elektrotechnik, Arbeitskreis Mess- und Informationstechnik, Rostock, Germany*, pp. 51–54, 2004.

[13] M. F. Hamilton and D. T. Blackstock, Eds., *Nonlinear Acoustics*, Academic Press, 1998.

[14] H. O. Berktay, "Possible exploitation of nonlinear acoustics in underwater transmitting applications," *Journal of Sound and Vibration*, vol. 2, no. 4, pp. 435–461, 1965.

[15] M. Crocker, *Handbook of Acoustics*, John Wiley & Sons, Inc, 1998.

[16] P. J. Westervelt, "Scatering of sound by sound," *Journal of the Acoustical Society of America*, vol. 29, no. 2, pp. 199–203, 1957.

[17] F. Giri and M. Morari E.-W. BaiM. Thoma, F. Allgwer, Eds., *Block-oriented Nonlinear System Identification*, Springer, 2010.